Genetically Optimization of an Asymmetrical Fuzzy Logic Based Photovoltaic Maximum Power Point Tracking Controller

Ammar AL-GIZI[1,2], Sarab AL-CHLAIHAWI[1], Mohamed LOUZAZNI[3], Aurelian CRACIUNESCU[1]
[1]*Electrical Engineering Faculty, University Politehnica of Bucharest, 060042, Romania*
[2]*Electrical Engineering Department, Al-Mustansiriyah University, Baghdad, 10001, Iraq*
[3]*National School of Applied Sciences (ENSA), Abdelmalek Essaadi University, 1818, Morocco*
ammar.ghalib@ieee.org

***Abstract*—This paper introduces a new fuzzy logic controller (FLC) based photovoltaic (PV) maximum power point tracking (MPPT) optimized with the genetic algorithm (GA). Four FLCs with five and seven numbers of triangular (tri) and generalized bell (g-bell) membership functions (MFs) are analyzed. The performances of the analyzed algorithms have been compared with the appropriate performances of the classical perturb and observe (P&O) algorithm by using the following criteria: the rise time (t_r), the tracking accuracy of the output power, and the energy yield. The results showed that the FL-based PV MPPT controller with seven triangular (7-tri) MFs provides the best steady-state performances.**

***Index Terms*—fuzzy logic, genetic algorithms, maximum power point trackers, optimization, photovoltaic systems.**

I. Introduction

In Photovoltaic (PV) systems, Maximum Power Point Tracking (MPPT) controllers are used to maximize the captured solar energy when the solar irradiation and cell temperature have the large variations during the time [1]. Some of very frequently PV MPPT algorithms used in this aim are: perturb and observe (P&O) algorithm, incremental conductance (InC) algorithm, and fuzzy logic (FL) algorithm [2-11]. In comparison with the conventional P&O algorithm, the FL algorithm with symmetrical membership functions (MFs) can simultaneously enhance the performances of the PV system both in terms of tracking speed and, also, in tracking accuracy [2-8]. The performance of the PV system can be further improved by using a FLC with five asymmetrical triangular MFs, in which the MFs' setting values are determined according to the characteristic of the PV power-voltage (*P-V*) curve [7, 8]. Since the MFs' setting values play an important influence on the PV MPPT effectiveness, many evolutionary algorithms, as GA and PSO, are recommended in the literature to optimize the MFs' choosing, instead of the trial and error approach [8],[12-14]. The FLC with five asymmetrical triangular MFs which is optimized by PSO method satisfies the best dynamic and steady tracking performances of the PV system, compared with a FLC of symmetrical MFs, and with P&O based MPPT methods [8]. In this paper, four new FL-based PV MPPT controllers with, respectively, five and seven asymmetrical triangular and g-bell type MFs are analyzed. The MFs' setting values, for each analyzed PV MPPT FLC, are optimally established by the GA. Finally, the performances of the FL-based PV MPPT controllers with asymmetrical MFs optimal settled and those of the traditional P&O algorithm are compared in terms of tracking speed, tracking accuracy, and an extracted energy.

II. Modeling of the PV System

In this paper, the Sanyo VBHN220AA01 PV module, with a maximum power of 220 W at standard technical condition (STC), is modeled. The utilized PV module consists of *N*s =72 series joined solar cells.

Appendix A lists the parameters of the utilized PV module [8]. The solar irradiation (*G*) and cell temperature (*T*) are the two essential factors that influence the output power delivered from the PV module [11]. A MPPT method is used to improve the performance of the overall PV system. The simple structure of the PV system with the FL-based MPPT control is shown in Fig. 1.

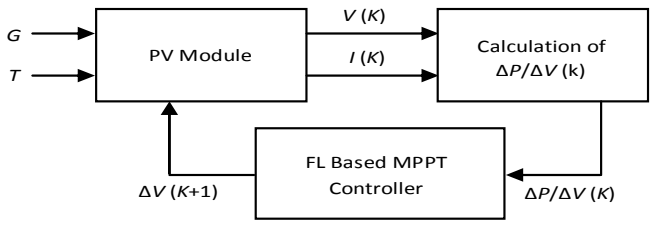

Figure 1. PV system with the FL-based MPPT controller

The mathematical model of the PV cell can be expressed as:

$$I = I_{ph} - I_o \cdot \left[\exp\left(\frac{q \cdot (V + I \cdot R_s)}{n \cdot K \cdot T} \right) - 1 \right] - \frac{V + I \cdot R_s}{R_{sh}}, \quad (1)$$

where V and I are a voltage and current of the PV cell, respectively. I_{ph} is the photocurrent. R_s and R_{sh} are the series and parallel resistances of the PV cell, respectively. I_o is the diode's reverse saturation current, q is the electron charge (1.602×10^{-19} C), K is the Boltzmann's constant (1.381×10^{-23} J/K), and n is the diode ideality factor [3, 4].

Fig. 2a shows the current-voltage (*I-V*) and power-voltage (*P-V*) curves of the utilized Sanyo VBHN220AA01 PV module at different *G* and *T* conditions simulated by Matlab software. The corresponding $\Delta P/\Delta V$ curves at different *G* are also described in Fig. 2b. It is clear from Fig. 2b that the $\Delta P/\Delta V$ of the utilized module changed smoothly; hence, it can be used as a proper input for the proposed FL-based MPPT controller.

Digital Object Identifier 10.4316/AECE.2017.04009

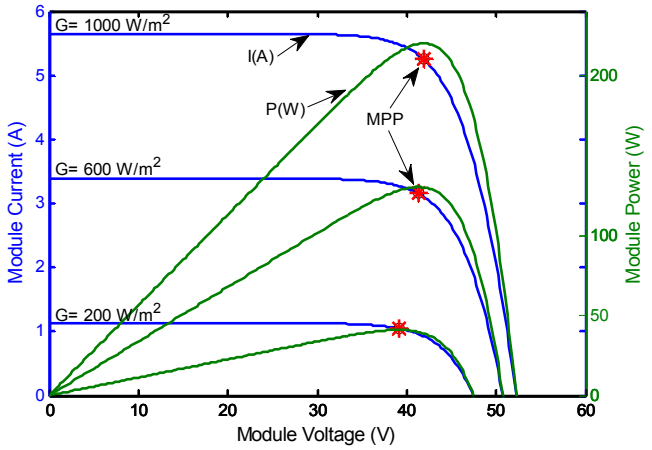

(a)

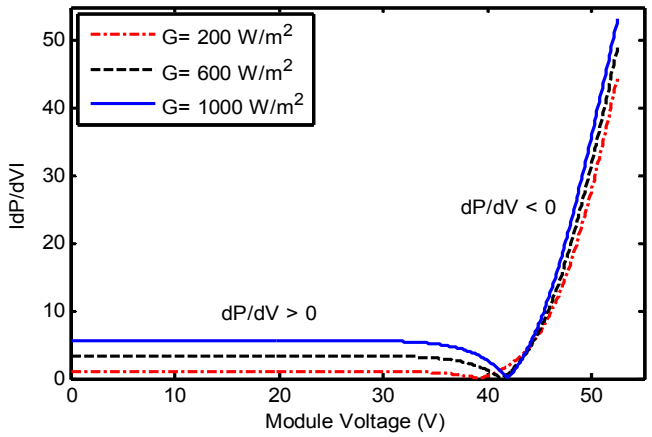

(b)

Figure 2. Characteristics of the utilized PV module at various irradiations and 25 ºC of temperature: (a) *I-V* and *P-V* curves; (b) |d*P*/d*V*| curves

III. FL-BASED MPPT CONTROLLER

The FLC is used to find and track the MPP of the PV system by producing the suitable voltage variation (perturbation step size). The basic stages of the proposed asymmetrical FL-based MPPT controller are illustrated in Fig. 3. The stages include; fuzzification with input MFs of linguistic labels, fuzzy inference engine, rule-base (RB), and defuzzification with output MFs [15, 16].

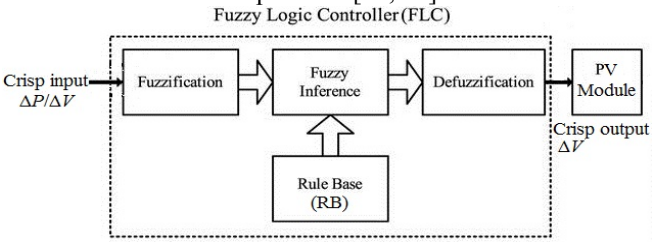

Figure 3. Stages of the proposed FL-based MPPT controller

In this paper, the input variable of the proposed FL-based MPPT controller is the power slope ($\Delta P/\Delta V$) whereas, the corresponding output variable is the voltage perturbation command (ΔV). For the FLC, the MFs of the input and output variables can be in triangular, generalized bell, Gaussian, trapezoidal, and sigmoidal forms with a different number of fuzzy sets (FS). According to the proposed FLC, two types of MFs are used: triangular and generalized bell shapes. For each type, five and seven FS are comprised. Consequently, four categories of the proposed FL-based MPPT controller are used: triangular MFs of five FS (5-tri), triangular MFs of seven FS (7-tri), generalized bell MFs of five FS (5-gbell), and generalized bell MFs of seven FS (7-gbell). Fig. 4 shows these MFs of the FLC input and output variables, where the symbols N, P, Z, S, M, and B are denoted as negative, positive, zero, small, medium, and big, respectively.

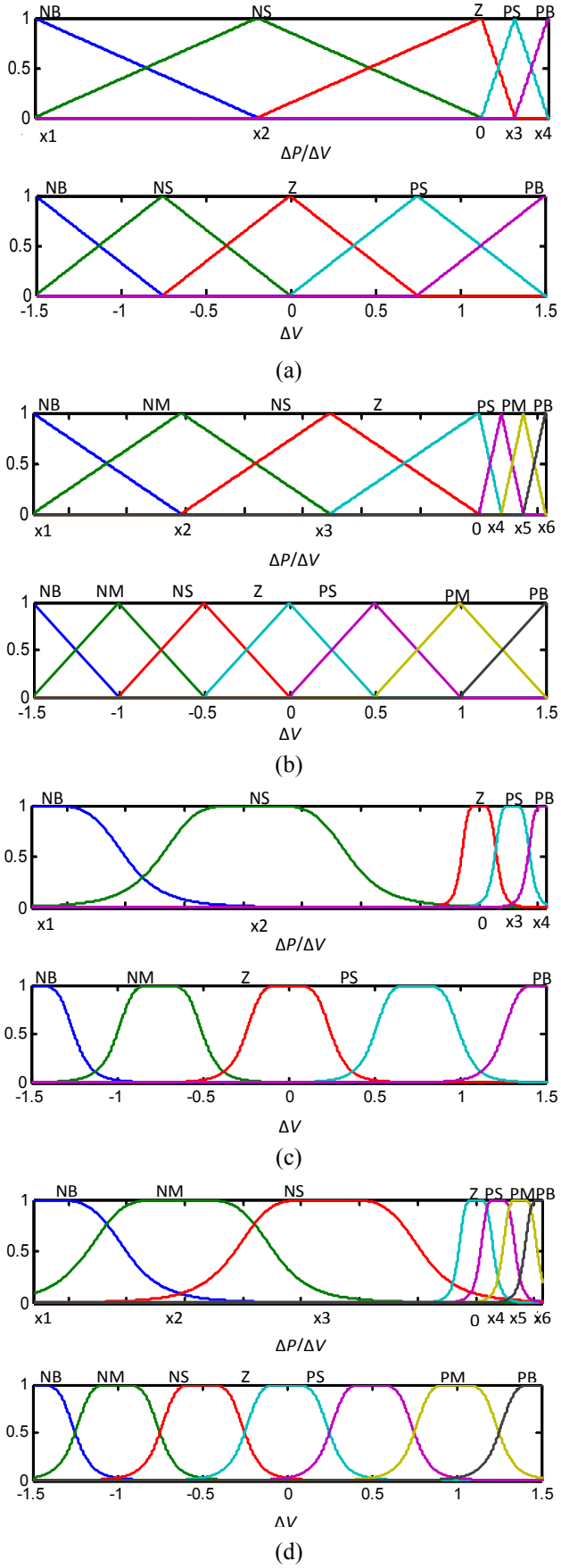

Figure 4. Asymmetrical MFs of the FLC input, $\Delta P/\Delta V$ and output, ΔV variables: (a) 5-tri; (b) 7-tri; (c) 5-gbell; (d) 7-gbell

According to the input $\Delta P/\Delta V$ of five MFs shown in Fig. 4a and Fig. 4c, RB of the proposed FLC includes five rules. Whereas for $\Delta P/\Delta V$ of seven MFs, the RB includes seven rules. Since $\Delta P/\Delta V$ is used as the input and ΔV is taken as the output; these rules are constructed based on the relationships between these variables. Table I and Table II show the RB for the proposed FLC based on five and seven MFs, respectively.

TABLE I. FUZZY RULE BASE TABLE BASED ON FIVE MFS

$\Delta P/\Delta V$	NB	NS	Z	PS	PB
ΔV	NB	NS	Z	PS	PB

TABLE II. FUZZY RULE BASE TABLE BASED ON SEVEN MFS

$\Delta P/\Delta V$	NB	NM	NS	Z	PS	PM	PB
ΔV	NB	NM	NS	Z	PS	PM	PB

At cell temperature of 25 °C, the typical *P-V* curves of the utilized PV module at 200 W/m^2 and 1000 W/m^2 of solar irradiations are illustrated in Fig. 5. According to Fig. 5, the sign and magnitude of the FLC output variable ΔV can be determined the sign and magnitude of the FLC input $\Delta P/\Delta V$ based on the following six operating conditions:

- Positive big $\Delta P/\Delta V$ indicates that the operating point locates on the left side and far from the MPP (point A in Fig. 5). Consequently, a larger ΔV is needed to fastly reach the MPP.
- Positive small $\Delta P/\Delta V$ indicates that the operating point locates on the left side and close to the MPP (point B in Fig. 5). Consequently, a smaller positive ΔV is needed to reach the MPP with minimum oscillation (ripple).
- Negative big $\Delta P/\Delta V$ indicates that the operating point locates on the right side and far from the MPP (point C in Fig. 5). Consequently, a larger negative ΔV is needed to rapidly reach the MPP.
- Negative small $\Delta P/\Delta V$ indicates that the operating point locates on the right side and close to the MPP (point D in Fig. 5). Consequently, a smaller negative ΔV is needed to reach the MPP with minimum oscillation (ripple).
- A zero $\Delta P/\Delta V$ indicates that the operating point locates on the MPP (MPP1 or MPP2 in Fig. 5). Consequently, a zero ΔV is needed to keep the position of the operating point on the MPP.
- A zero ΔV and positive ΔP due to an increase in the solar irradiation indicates that the operating point is suddenly jumped from MPP1 to point E as shown in Fig. 5. Hence, a positive ΔV is required to reach the MPP2 which is shown in Fig. 5. Vice versa, when ΔV is zero and ΔP is negative due to a solar irradiation decrease, the operating point moves from MPP2 to point F as shown in Fig. 5. Hence, a negative ΔV is required to reach the MPP1 as shown in Fig. 5.

The final process of the FLC is the defuzzification. The center of gravity (COG) method used for the defuzzification can be represented by [17-19]:

$$\Delta V = \frac{\sum_{i=1}^{n} (\Delta V_i \times \mu(\Delta V_i))}{\sum_{i=1}^{n} \mu(\Delta V_i)} \quad (2)$$

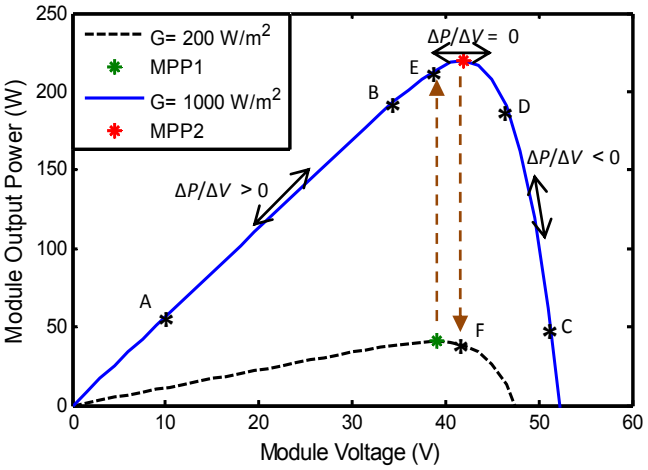

Figure 5. *P-V* curves of Sanyo VBHN220AA01 PV module

IV. DESIGN OF AN ASYMMETRICAL FLC-BASED MPPT

The design of MF setting values plays a vital role in the design of the proposed FL-based MPPT controller. For the universe of discourse (UOD) of the FLC output ΔV, symmetrical MFs of fixed maximum boundaries of ±1.5 V were used, as shown in Fig. 4.

At a fixed voltage variation (ΔV), it can be seen from Fig. 2 that the $\Delta P/\Delta V$ on the two sides of the MPP are dissimilar. Since $\Delta P/\Delta V$ is larger on the right side than its value on the left side of the MPP, the UOD of the FLC input $\Delta P/\Delta V$ should be asymmetrical. Fig. 6 explains the main principle for deriving the MF setting values of dP/dV based on STC. For the utilized Sanyo VBHN220AA01 PV module, by increasing the module voltage (V) from short circuit voltage (0 V) to open circuit voltage (52.3 V) using a fixed ΔV of 1.5 V, the curve resulted in Fig. 6 can be obtained.

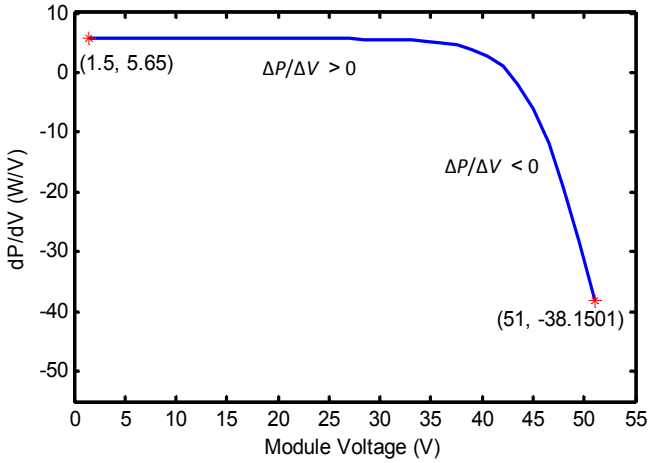

Figure 6. Principle of deriving the MF setting values of dP/dV

It can be seen from Fig. 6 that the maximum positive value of dP/dV (left side of the MPP) is 5.65 W/V, whereas the maximum negative value of dP/dV (right side of the MPP) is 38 W/V. Consequently, the negative boundary of dP/dV (x1 in Fig. 4), should be equal 38/5.65 times of the positive boundary of dP/dV (x4 and x6 in Fig. 4). Hence, the value of x1 is -38, whereas the value of x4 and x6 is 5.65.

To further enhance the performance of the proposed asymmetrical FL-based MPPT controller, the MF setting values of dP/dV can be further optimized. In this paper, the GA optimization method is used, as it is explained in the next section.

V. Optimization of Asymmetrical FLC Using GA

According to the number of MFs which are used in the input variable d*P*/d*V* of the FL-based MPPT controller, the MF setting values that should be optimized is decided. From Fig. 4, in the case of five MFs, there are four setting values: x1, x2, x3, and x4 that should be optimized. In contrast, in the case of seven MFs, there are six setting values: x1, x2, x3, x4, x5 and x6 that should be optimized.

The GA, which is chosen to optimize these MF setting values of d*P*/d*V*, is presented as follows:

A. Optimizing the MF Setting Values of ΔP/ΔV Using GA

The optimization problem for the setting values based on five MFs can be written as:

Maximize fitness function f(x1, x2, x3, x4), subjected to the constraints:

$x1 < x2 < 0$,
$0 < x3 < x4$,
$x1 > NE_{max}$,
$x4 < PO_{max}$

Whereas, for the setting values based on seven MFs, the optimization problem can be written as:

Maximize fitness function f(x1, x2, x3, x4, x5, x6), subjected to:

$x1 < x2 < x3 < 0$,
$0 < x4 < x5 < x6$,
$x1 > NE_{max}$,
$x6 < PO_{max}$

Where, for the optimization process, PO_{max} and NE_{max} are the maximum positive and negative limits, respectively.

GA is a part of evolutionary computing, which is a rapidly growing area of artificial intelligence (AI) [20-23]. The flow chart of a simple GA is shown in Fig. 7.

From Fig. 7, the optimization steps of the GA to optimize the MF setting values of $\Delta P/\Delta V$ can be illustrated by the following five steps:

1) Encoding

In this paper, a real-coded is used to encode the strings (chromosomes) of each population. The chromosome is a vector of four parameters (in the case of five MFs) and six parameters (in the case of seven MFs).

In the case of five MFs which are shown in Fig. 4, the four parameters of an initial chromosome can be chosen as:

x1=-38, x2=-19, x3=2.825, and x4=5.65.

Consequently, for seven MFs, the six parameters of initial chromosome can be chosen as:

x1=-38, x2=-25.33, x3=-12.67, x4=1.88, x5=3.77, and x6=5.65.

In this paper, the chosen values of PO_{max} and NE_{max} are 12 and -76, respectively.

For the population of ten chromosomes (chosen in this paper), the remaining chromosomes are initiated randomly, with each gene should satisfy the above inequality constraints.

2) Simulation and fitness evaluation

According to parameters of each chromosome, simulation is performed for the proposed FL-based MPPT controller at STC. In this paper, the initial operating point is located at the left side of MPP on the *P-V* curve with initial module voltage of 1.5 V (less than 3% of V_{oc}). Subsequently, simulation results are used to evaluate the required fitness function. The aim of the optimization process is to maximize the extracted power from the utilized PV module and minimize the rising time of MPPT. Hence, the fitness function (cost function) which is blended with 30% transient response and 70% steady state response is used. This fitness function can be defined as [8]:

$$Fitness = \left[0.3 \cdot \left(\frac{t_f - t_r}{t_f} \right) + 0.7 \cdot \frac{\int_{t_r}^{t_f} V(t) \cdot I(t)\, dt}{\int_{t_r}^{t_f} P_{MPP}\, dt} \right] \times 100\%, \quad (3)$$

where t_r is the rise time which is the time required for the output power to go from 10% to 90% of its final value, whereas t_f is final simulation time [8, 24]. These parameters are illustrated in Fig. 8.

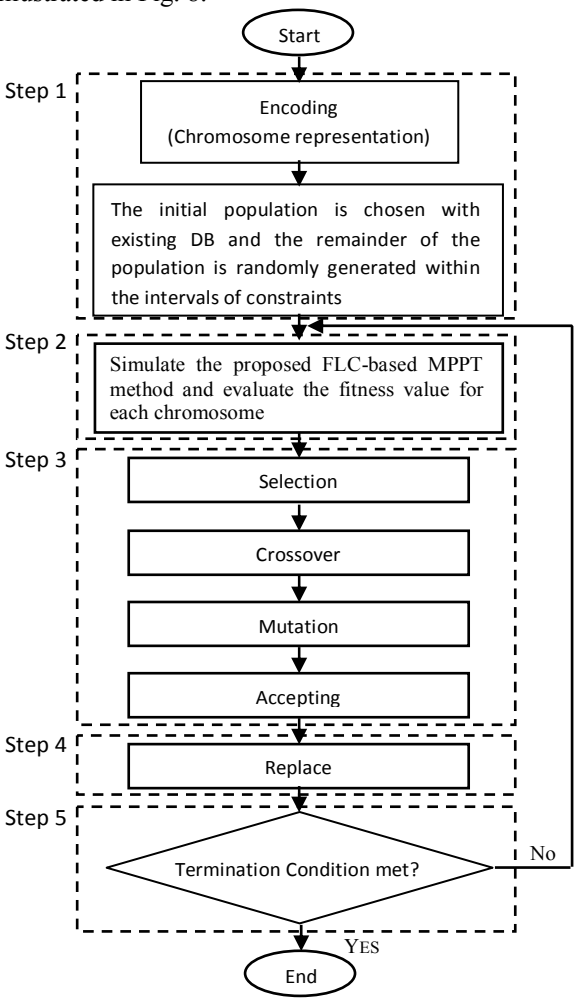

Figure 7. The flow chart of a simple GA

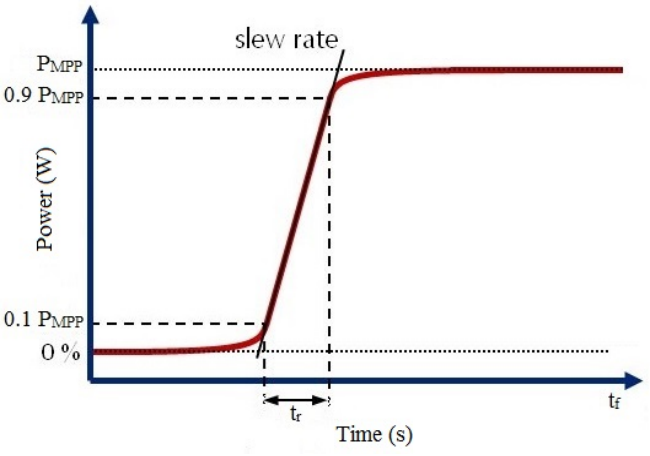

Figure 8. Concept of the utilized fitness function evaluation

From (3), the numerator of the steady-state response part represents the possible extracted energy during the time period from t_r to t_f, whereas, the denominator of this part represents the maximum available energy during this time period. A higher fitness value indicates that the better performance is obtained [9, 11].

3) New population

By applying the GA operations; selection, crossover, mutation, and accepting, the chromosome that gives high fitness value will be survived. Hence, a new population will be created [17-19]. In this paper, the following GA parameters are utilized during the optimization process:

- The roulette wheel method is used for selection.
- Multi-point (2 points) crossover type with a probability of 95% is used.
- Uniform mutation type with a probability of 1% is used.

4) Replace

After the mutation, the newly generated population is used. Moreover, an elitist strategy is used in this step. This strategy permits the best solution for a given generation to be directly used in the next generation.

5) Test the termination condition

In this paper, the maximum allowable generation number of 50 is used as a termination condition. If this termination condition satisfies, the optimization algorithm will be stopped; otherwise, the generation number will be increased by 1 and jumps to step 2, as shown in Fig. 7.

VI. Simulation Results

To prove the activity of the proposed MPPT method, simulations during 30 s with sampling time of 0.1 s are executed using; well-known conventional P&O which is developed in [2-6], asymmetrical FLC-based MPPT of different type and number of MFs which is explained in section IV, and GA optimized FLC-based MPPT which is explained in section V. Table III illustrates the setting values of the different MPPT methods. Consequently, the MF setting values of asymmetrical and optimized FLC-based MPPT methods are shown in Fig. 9 and Fig. 10, respectively.

TABLE III. Setting Values of the MPPT Methods

MPPT Method	Setting Value
P&O (ΔV=0.5 V)	Fixed Voltage Variation
P&O (ΔV=5 V)	Fixed Voltage Variation
Asymmetrical FLC of 5 MFs	x1= -38 x2= -19 x3= 2.825 x4= 5.65
Asymmetrical FLC of 7 MFs	x1= -38 x2= -25.33 x3= 12.67 x4= 1.88 x5= 3.77 x6= 5.65
Optimized FLC (5-tri)	x1= -45.21 x2= -2.422 x3= 1.2 x4= 4.32
Optimized FLC (7-tri)	x1= -34.52 x2= -23.43 x3= -1.84 x4= 1.38 x5= 3.53 x6= 5.01
Optimized FLC (5-gbell)	x1= -38 x2= -19 x3= 1.445 x4= 5.65
Optimized FLC (7-gbell)	x1= -38.97 x2= -19.95 x3= -18.15 x4= 1.92 x5= 3.2 x6= 5.84

To highlight the improvement of the different asymmetrical FLC-based MPPT methods, Fig. 12 shows the power output and energy yield of the utilized PV module using these MPPT methods at STC. Furthermore, the power output and energy yield of the utilized PV module using the GA optimized FL-based MPPT controllers of different type and the numbers of MFs are illustrated in Fig. 13.

For further comparison of the MPPT methods; rise time (t_r), tracking accuracy, energy yield, and fitness function value are calculated during the simulation time. Table IV clarify the comparative results of the different MPPT methods, taking into consideration that the expected maximum power and energy yield of the utilized PV module at STC are 219.9751 W and 1.8331 Wh, respectively.

In the case of a voltage perturbation of 5 V, the tracking speed of P&O is the fastest compared with the other MPPT methods, as shown in Fig. 12a, where, t_r of P&O (ΔV=5 V) is 0.7 s, whereas the t_r of P&O (ΔV=0.5 V), asymmetrical FLC (5-tri), asymmetrical FLC (7-tri), asymmetrical FLC (5-gbell), and asymmetrical FLC (7-gbell) are 6.8 s, 2.8 s, 2.6 s, 2.8 s, and 3.1 s, respectively. Although the tracking speed is increased, the tracking accuracy (94.7934%) is deteriorated due to a large oscillation of the operating point around the MPP, as shown in Fig. 12a. vice versa, in the case of P&O (ΔV=0.5 V), the tracking accuracy is improved (99.7232%) but the tracking speed is decreased (t_r=6.8 s). Hence, the proposed asymmetrical FLC-based MPPT methods regardless of type and number of used MFs can successfully improve the tracking accuracy and speed performance of the utilized PV module simultaneously, as shown in Fig. 12a. Moreover, it can be seen from Fig. 12a and Table IV that the asymmetrical FLC of seven triangular (7-tri) MFs has the best tracking speed and accuracy over the others asymmetrical FL-based MPPT methods. Consequently, the PV system with this type of the proposed MPPT method can deliver more energy (1.7531 Wh) than the other types of asymmetrical FLC-based MPPT methods, as shown in Fig. 12b and Table IV. Where the energy yields in case of asymmetrical FLC-based on 5-tri, 5-gbell, and 7-gbell are 1.7475 Wh, 1.7461 Wh, and 1.7362 Wh, respectively. For the optimized FLC-based MPPT method by GA, the optimized FLC of 7-tri MFs also performs the best results among the other types of optimized FLC methods. Where, its improvements over the optimized FLC of 5-tri MFs in terms of tracking accuracy, energy yield, and fitness function values are 0.025%, 0.3%, and 0.123%, respectively, as shown in Fig. 13 and Table IV.

On the other hand, by comparing the results of GA optimized FLC of 7-tri MFs with the asymmetrical FLC of 7-tri MFs, it can be seen that the improvements which are added by the optimization are inconspicuous. These improvements in terms of tracking accuracy, energy yield, and fitness function values are 0.021%, 0.03%, and 0.02%, respectively, as shown in Table IV. From Table IV, the proposed FLC method of 7-tri MFs has the largest fitness function, which means that the type and number of MFs has a positive effect on the performance of the MPPT method. On the other hand, the optimization performance based on the GA for the 5-tri MFs is shown in Fig. 11. It is obvious from Fig. 11 that the maximum fitness value of 0.9176 can be achieved at generation number 13 of 50.

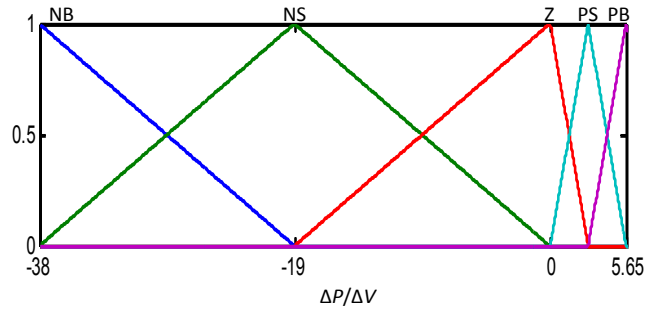

(a)

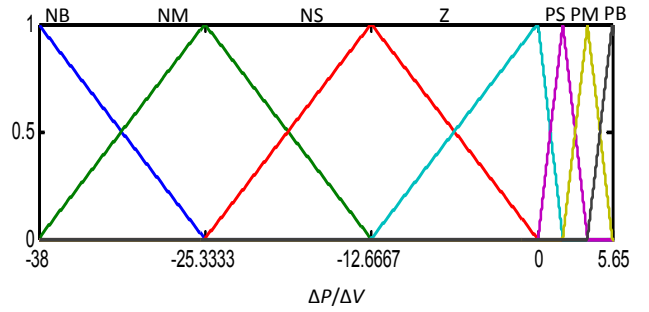

(b)

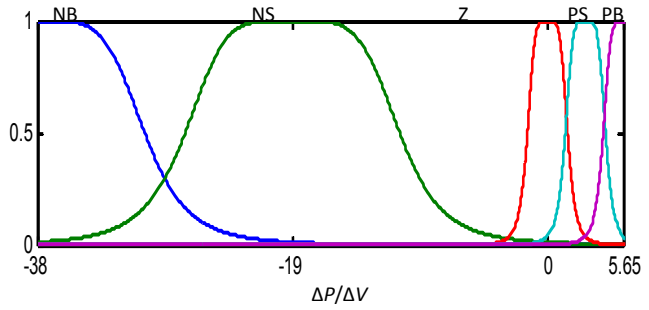

(c)

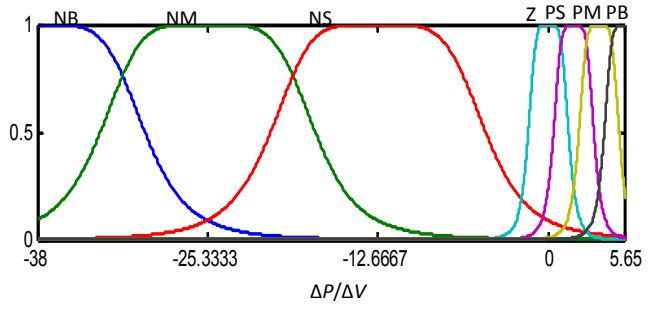

(d)

Figure 9. MF setting values of $\Delta P/\Delta V$ for asymmetrical FLC-based MPPT: (a) 5-tri; (b) 7-tri; (c) 5-gbell; (d) 7-gbell

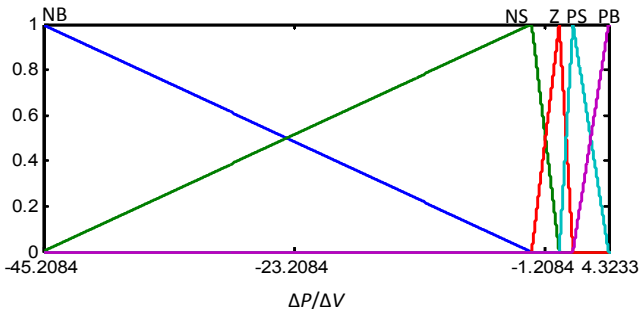

(a)

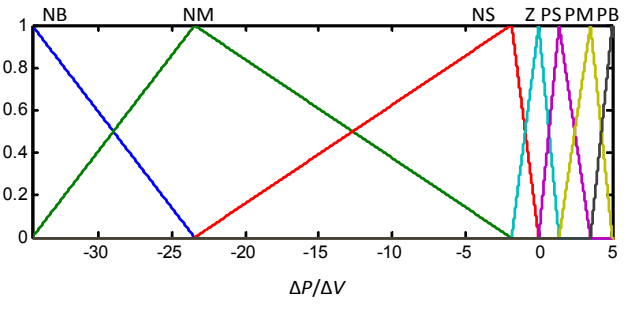

(b)

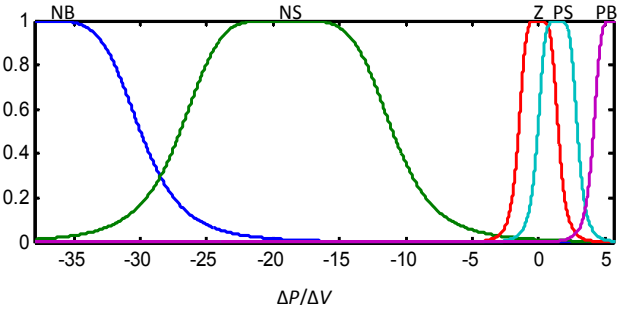

(c)

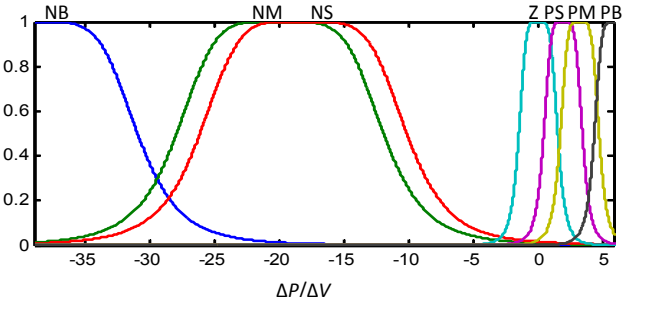

(d)

Figure 10. MF setting values of $\Delta P/\Delta V$ for optimized FLC-based MPPT: (a) 5-tri; (b) 7-tri; (c) 5-gbell; (d) 7-gbell

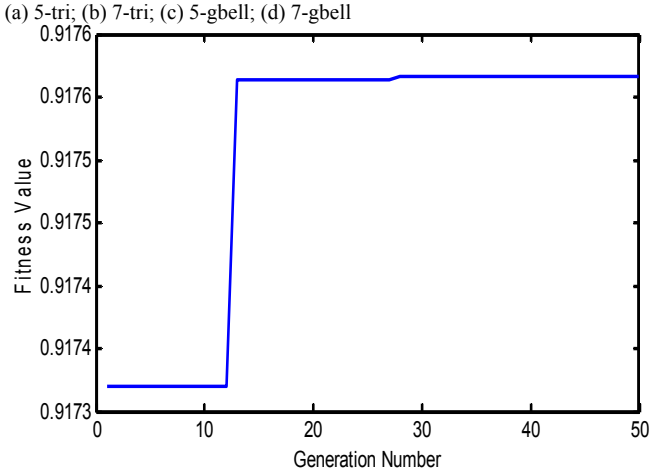

Figure 11. Optimization performance of GA

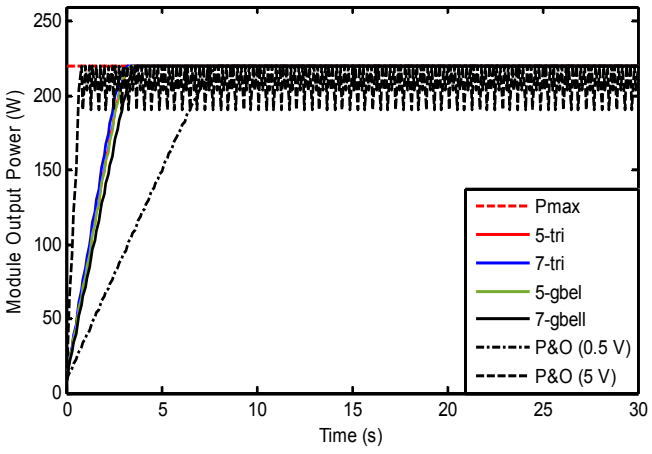

(a)

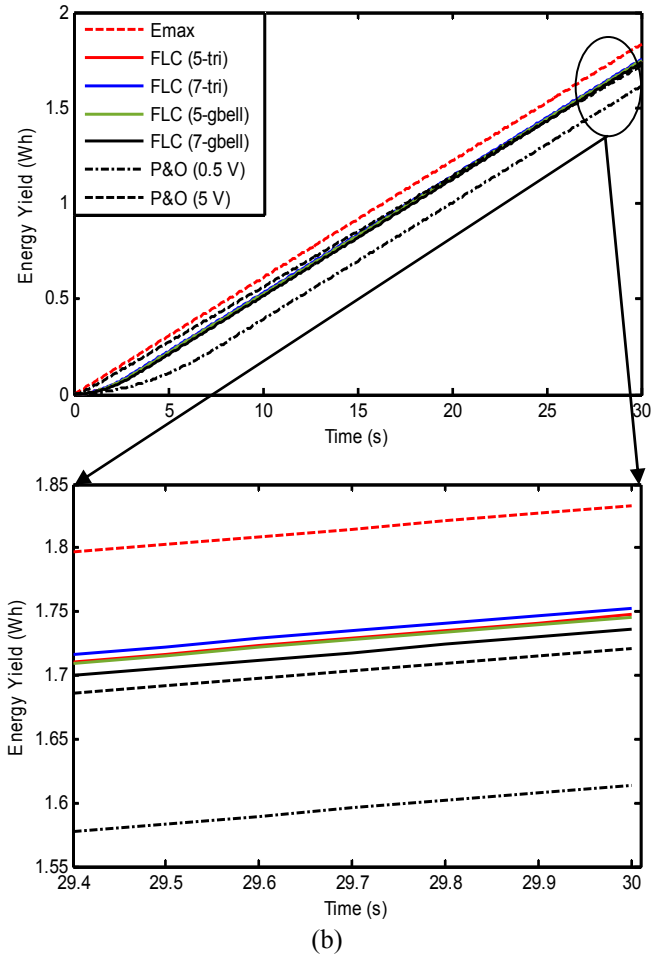

(b)

Figure 12. Output power and energy yield of the PV module using P&O and asymmetrical FLC-based MPPT methods at STC: (a) Power; (b) Energy yield

TABLE IV. PERFORMANCE OF THE MPPT METHODS AT STC

MPPT Method	Average Steady-State Power (W)	MPPT Accuracy (%)	Rise Time t_r (s)	Energy Yield (Wh)	Fitness Value
P&O (ΔV=0.5 V)	219.366	99.723	6.8	1.614	0.930
P&O (ΔV=5 V)	208.522	94.793	0.7	1.721	0.956
Asymmetrical FLC (5-tri)	219.781	99.912	2.8	1.747	0.971
Asymmetrical FLC (7-tri)	219.790	99.916	2.6	1.753	0.973
Asymmetrical FLC (5-gbell)	219.711	99.879	2.8	1.746	0.971
Asymmetrical FLC (7-gbell)	219.728	99.888	3.1	1.736	0.968
Optimized FLC (5-tri)	219.782	99.912	2.7	1.748	0.972
Optimized FLC (7-tri)	219.836	99.937	2.6	1.754	0.974
Optimized FLC (5-gbell)	219.053	99.581	2.6	1.745	0.971
Optimized FLC (7-gbell)	219.519	99.792	2.8	1.744	0.970

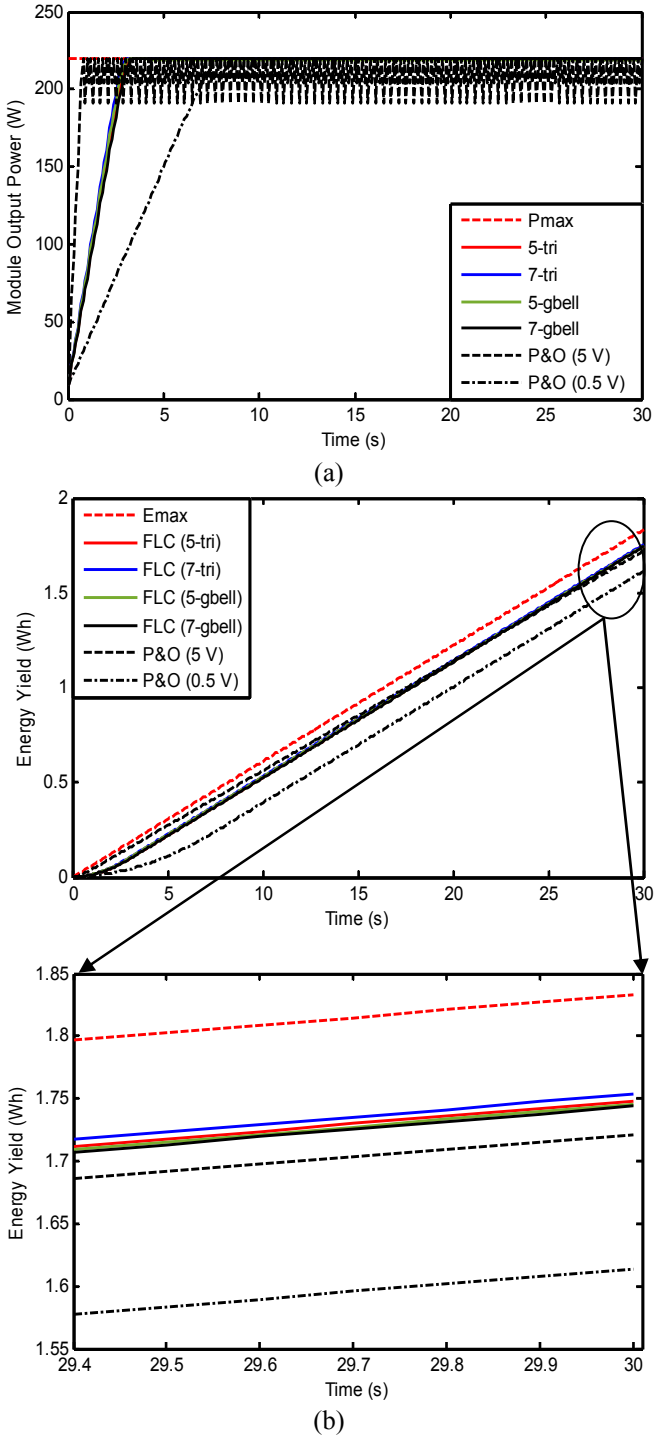

(a)

(b)

Figure 13. Output power and energy yield of the PV module using P&O and GA optimized FLC-based MPPT methods at STC: (a) Power; (b) Energy yield

VII. CONCLUSION

In this paper, an asymmetrical FLC-based MPPT method for PV system is presented using different numbers and types of MFs. Moreover, GA optimization method is used to optimize the parameters of the different types input MFs.

During 30 s of the simulation time, although the P&O (ΔV=5 V) has the best tracking speed with lowest t_r of 0.7 s among the other MPPT methods, the tracking accuracy is clearly decreased, as shown in Fig. 12a, Fig. 13a, and Table IV. Hence, PV system with the conventional P&O method can harvests the least energy compared with the other tracking methods, as shown in Fig. 12b, Fig. 13b, and Table IV.

According to the comparative study of the different MPPT methods, the fitness function values of the asymmetrical FLC-based MPPT methods are higher than that of the conventional P&O based MPPT method, as shown in Table IV. Moreover, the asymmetrical FLC of 7-tri MFs is the best among the other types of asymmetrical FLC methods in terms of rising time, tracking accuracy, and energy yield, as shown in Fig. 12 and Table IV. In the same manner, the GA optimized FLC-based MPPT methods have superior fitness values than those of the conventional P&O and other types of asymmetrical FLC methods. Furthermore, it can be concluded that the improvement added by the optimized FLC-based MPPT methods is insignificant. Compared with the asymmetrical FLC of 7-tri MFs, the optimized FLC of 7-tri MFs can improve the tracking accuracy, energy yield, and fitness function value only by 0.021%, 0.03%, and 0.02%, respectively, as shown in Table IV. Hence, although the GA cannot guarantee to satisfy the optimal MF setting values, it can enhance the performance of the asymmetrical FLC-based MPPT controller without increasing in the implementation complexity. Moreover, it can be concluded that the selection of MF's type and number in the design of FLC-based MPPT method can improve the overall performance of the PV system.

APPENDIX A

The parameters of SANYO VBHN220AA01 PV module at STC: maximum power P_{max}= 220 W, maximum power voltage V_{mpp}= 42.7 V, maximum power current I_{mpp}= 5.17 A, open-circuit voltage V_{oc}= 52.3 V, short-circuit current I_{sc}= 5.65 A, and temperature co-efficient α_v= -0.336%/^{o}C.

REFERENCES

[1] S. Saravanan, R. Babu, "Maximum power point tracking algorithms for photovoltaic system- a review," Renewable and Sustainable Energy Reviews, vol. 57, pp. 192-204, 2016. doi: 10.1016/j.rser.2015.12.105

[2] T. M. Mohan, V. Vakula, "Comparative analysis of perturb & observe and fuzzy logic maximum power point tracking techniques for a photovoltaic array under partial shading conditions," Leonardo Journal of Sciences, vol. 27, pp. 1-16, Jul. 2015.

[3] A. G. Al-Gizi and S. J. Al-Chlaihawi, "Study of FLC based MPPT in comparison with P&O and InC for PV systems," in Proc. of IEEE International Symposium on Fundamentals of Electrical Engineering (ISFEE 2016), Bucharest, Romania, 2016, pp. 1-6. doi: 10.1109/ISFEE.2016.7803187

[4] A. G. Al-Gizi, "Comparative study of MPPT algorithms under variable resistive load," in Proc. of IEEE International Conference on Applied and Theoretical Electricity (ICATE 2016), Craiova, Romania, 2016, pp. 1-6. doi: 10.1109/ICATE.2016.7754611

[5] A. M. Othman, M. M. El-Arini, A. Ghitas, A. Fathy, "Realworld maximum power point tracking simulation of PV system based on fuzzy logic control," NRIAG Journal of Astronomy and Geophysics, vol. 1, no. 2, pp. 186-194, 2012. doi: 10.1016/j.nrjag.2012.12.016

[6] F. L. Tofoli, D. de Castro Pereira, W. J. de Paula, "Comparative study of maximum power point tracking techniques for photovoltaic systems," International Journal of Photoenergy, vol. 2015, pp. 1-10, Jan. 2015. doi: 10.1155/2015/812582

[7] C. L. Liu, J. H. Chen, Y. H. Liu, Z. Z. Yang, "An asymmetrical fuzzy-logic-control-based MPPT algorithm for photovoltaic systems," Energies, vol. 7, no. 4, pp. 2177-2193, Apr. 2014. doi: 10.3390/en7042177

[8] P. C. Cheng, B. R. Peng, Y. H. Liu, Y. S. Cheng, J. W. Huang, "Optimization of a fuzzy-logic-control-based MPPT algorithm using the particle swarm optimization technique," Energies, vol. 8, no. 6, pp. 5338-5360, 2015. doi: 10.3390/en8065338

[9] N. Altin, "Interval type-2 fuzzy logic controller based maximum power point tracking in photovoltaic systems," Advances in Electrical and Computer Engineering, vol. 13, no. 3, pp. 65-70, 2013. doi: 10.4316/AECE.2013.03011

[10] A. Durusu, I. Nakir, A. Ajder, R. Ayaz, H. Akca, M. Tanrioven, "Performance comparison of widely used maximum power point tracking algorithms under real environmental conditions," Advances in Electrical and Computer Engineering, vol. 14, no. 3, pp. 89-94, 2014. doi: 10.4316/AECE.2014.03011

[11] D. Petreus, D. Moga, A. Rusu, T. Patarau, M. Munteanu, "Photovoltaic system with smart tracking of the optimal working point," Advances in Electrical and Computer Engineering, vol. 10, no. 3, pp. 40-47, 2010. doi: 10.4316/AECE.2010.03007

[12] A. Rahma and M. Khemliche, "Combined approach between FLC and PSO to find the best MFs to improve the performance of PV system under variable climate conditions and load requirements," in Proc. of IEEE International Conference on Electrical Sciences and Technologies in Maghreb (CISTEM 2014), Nov. 3-6, 2014, pp. 1-8. doi: 10.1109/CISTEM.2014.7077038

[13] N. Hashim, Z. Salam, and S. M. Ayob, "Maximum power point tracking for stand-alone photovoltaic system using evolutionary programming," in Proc. of IEEE 8th International Power Engineering and Optimization Conference (PEOCO2014), Langkawi, Malaysia, 2014, pp. 7-12. doi: 10.1109/PEOCO.2014.6814390

[14] A. Messai, A. Mellit, A. Guessoum, S. A. Kalogirou, "Maximum power point tracking using a GA optimized fuzzy logic controller and its FPGA implementation," Solar Energy, vol. 85, no. 2, pp. 265-277, 2011.

[15] M. T. Guneser, E. Erdil, M. Cernat, T. Ozturk, "Improving the energy management of a solar electric vehicle," Advances in Electrical and Computer Engineering, vol. 15, no. 4, pp. 53-62, 2015. doi: 10.4316/AECE.2015.04007

[16] E. Sahin, I. H. Altas, "FPA tuned fuzzy logic controlled synchronous buck converter for a wave/sc energy system," Advances in Electrical and Computer Engineering, vol. 17, no. 1, pp. 39-48, 2017. doi: 10.4316/AECE.2017.01006

[17] A. G. Al-Gizi, "Multi-stages for tuning of fuzzy logic controller (FLC) using genetic algorithm (GA)," Eng. & Tech. Journal, vol. 31, no. 6, part A, pp. 1166-1181, 2013.

[18] A. G. Al-Gizi, E. A. Hussein, "FPGA-based implementation of genetically tuned fuzzy logic controller (GA-FLC)," Journal of Engineering and Development, vol. 16, no. 3, pp. 241-257, Sep. 2012.

[19] S. A. Al-Obaidi, M. N. Al-Tikriti, A. G. Al-Gizi, "Tuning of composite fuzzy logic guidance law using genetic algorithms," Eng. & Tech. Journal, vol. 30, no. 13, pp. 2341-2356, Jan. 2012.

[20] F. Herrera, L. Magdalena, "Genetic fuzzy systems: a tutorial," Tatra Mountains Mathematical Publications, vol. 13, pp. 93-121, Jun. 1997.

[21] P. Wang, D. P. Kwok, "Optimal design of PID process controllers based on genetic algorithms," Control Eng. Pract., vol. 2, no. 4, pp. 641-648, 1994.

[22] J. H. Van der Lee, W. Y. Svrcek, B. R. Young, "A tuning algorithm for model predictive controllers based on genetic algorithms and fuzzy decision making," ISA Trans., vol. 47, no. 1, pp. 53-59, 2008.

[23] B. Sarkar, P. Mandal, R. Saha, S. Mookherjee, D. Sanyal, "GA-optimized feed forward-PID tracking control for a rugged electrohydraulic system design," ISA Trans., vol. 52, no. 6, pp. 853-861, 2013.

[24] Matlab, Global Optimization Toolbox, "User's Guide (R2015b)," The MathWorks Inc., 2015.